Optically bright Active Galactic Nuclei in the ROSAT-Faint Source Catalogue[⋆]

M.-P. Véron-Cetty[1], S.K. Balayan[2], A. M. Mickaelian[2], R. Mujica[3], V. Chavushyan[3], S. A. Hakopian[2], D. Engels[4], P. Véron[1], F.-J. Zickgraf[4], W. Voges[5], D.-W. Xu[6,5]

[1] Observatoire de Haute Provence, CNRS, F-04870 Saint-Michel l'Observatoire, France
  e-mail: `mira.veron@oamp.fr; philippe.veron@oamp.fr`
[2] Byurakan Astrophysical Observatory and Isaac Newton Institute of Chile, Armenian branch, Byurakan 378433, Aragatzotn province, Armenia
  e-mail: `bal@moon.yerphi.am; aregmick@apaven.am; sanna@eugene.yerphi.am`
[3] INAOE, Apdo. postal 51 y 216, 72000 Puebla, Pue., Mexico
  e-mail: `rmujica@inaoep.mx; vahram@inaoep.mx`
[4] Hamburger Sternwarte, Gojenbergsweg 112, 21029 Hamburg, Germany
  e-mail: `dengels@hs.uni-hamburg.de; fzickgraf@hs.uni-hamburg.de`
[5] Max-Planck-Institute für extraterrestrische Physik, Postfach 1312, D-85741, Garching, Germany
  e-mail: `whv@mpe-garching.mpg.de`
[6] National astronomical observatories, Beijing 100012, China
  e-mail: `dwxu@bao.ac.cn`

Abstract. To build a large, optically bright, X-ray selected AGN sample we have correlated the ROSAT-FSC catalogue of X-ray sources with the USNO catalogue limited to objects brighter than O=16.5 and then with the APS database. Each of the 3 212 coincidences was classified using the slitless Hamburg spectra. 493 objects were found to be extended and 2 719 starlike. Using both the extended objects and the galaxies known from published catalogues we built up a sample of 185 galaxies with $O_{APS} < 17.0$ mag, which are high-probability counterparts of RASS-FSC X-ray sources. 130 galaxies have a redshift from the literature and for another 34 we obtained new spectra. The fraction of Seyfert galaxies in this sample is 20%. To select a corresponding sample of 144 high-probability counterparts among the starlike sources we searched for very blue objects in an APS-based color-magnitude diagram. Forty-one were already known AGN and for another 91 objects we obtained new spectra, yielding 42 new AGN, increasing their number in the sample to 83. This confirms that surveys of bright QSOs are still significantly incomplete. On the other hand we find that, at a flux limit of 0.02 count s^{-1} and at this magnitude, only 40% of all QSOs are detected by ROSAT.

Key words. Quasars: general, X-rays: AGN, Galaxies: Seyfert

February 2, 2008

1. Introduction

The ROSAT All-Sky Survey Bright Source Catalogue (RASS-BSC) is derived from the all-sky survey performed during the ROSAT mission in the energy band 0.1-2.4 keV; it contains 18 811 sources down to a limiting ROSAT-PSPC count-rate of 0.05 count s^{-1} (Voges et al. 1999). The 2 012 brightest (count-rate above 0.2 count s^{-1}) high galactic latitude (|b|>30°) sources of the BSC catalogue have been tentatively optically identified by Schwope et al.

(2000). The ROSAT Faint Source Catalogue (FSC)(Voges et al. 2000) contains 105 924 sources and represents the faint extension of the RASS-BSC.

The Hamburg QSO Survey is a wide-angle objective prism survey for finding bright QSOs in the northern sky. The survey plates have been taken with the former Hamburg Schmidt telescope now located at the Spanish-German Center in Calar Alto (Spain). A 1°.7 objective prism has been used providing unwidened spectra with a dispersion of 1 390 Å mm^{-1} at Hγ (Hagen et al. 1995). The slitless spectra allow the classification of objects brighter than about B=17.0. The first study of a sample of previously known QSOs with the *Einstein Observatory* has shown that, as a class, they are luminous X-ray emitters

---

[⋆] Tables 2, 3 and 4 are only available in electronic form at http://www.edpsciences.org

(Tananbaum et al. 1979). Bade et al. (1998) and Zickgraf et al. (2003) have described a way to identify X-ray sources by using the Hamburg survey plates; this process has been applied to a subsample of 5 341 sources from the ROSAT-BSC.

In the present paper we try to find all AGN brighter than O=16.5 in a subarea of the ROSAT-FSC. As the FSC survey is only about 2.5 times deeper than the BSC survey, we do not expect a significant difference in the identification content of these two samples but, because the number of sources in the FSC survey is much larger, we expect the discovery of many additional optically bright AGN. As the ROSAT survey is a low-energy survey, it contains a relatively high fraction of Narrow-Line Seyfert 1 Galaxies (NLS1s) because they usually have a soft X-ray excess (see for instance Laor et al. 1997); we therefore expect to find new bright NLS1s.

In the following we call AGN (or Active Galactic Nuclei) QSOs, BL Lac objects, Seyfert galaxies and Liners. QSOs are defined as Seyfert 1 galaxies brighter than $M_B=-23.0$[1] .

2. Analysis

2.1. The sample

In the area of the sky defined by $\delta > 0º$ and $|b| > 30º$ (10 313 deg^2) there are 29 321 ROSAT-FSC sources.
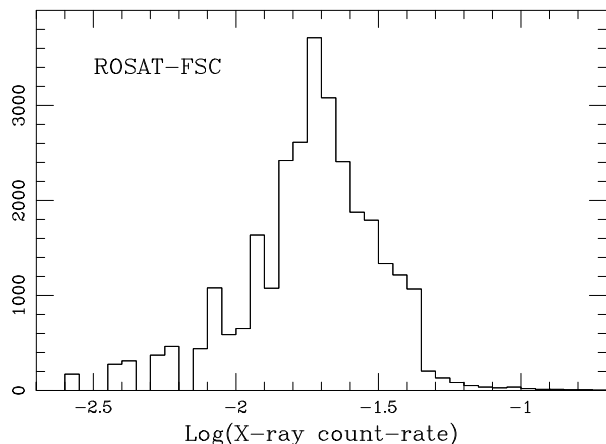

Fig. 1. Histogram of the logarithm of the X-ray count rates (in counts s^{-1}) of the 29 321 ROSAT-FSC sources.

Figure 1 shows the histogram of the logarithm of the X-ray count rates of these sources (in counts s^{-1}). Below 0.02 counts s^{-1} the survey is obviously quite incomplete, reflecting the fact that its sensitivity limit is not uniform over the sky. On the other hand 130 sources have a count rate greater than 0.05 counts s^{-1} but were not included in the BSC as their detected photon number was less than 15. They were included in the FSC.

[1] Throughout this work we used H$_o$=50 km s^{-1} Mpc^{-1} and q$_o$=0

Figure 2 shows the distribution over the sky of (a) the 29 321 sources and (b) the 15 848 sources with F$_x$ > 0.02 counts s^{-1}. The second distribution is much more uniform than the first and, in the following, we shall restrict our analysis to this subsample.
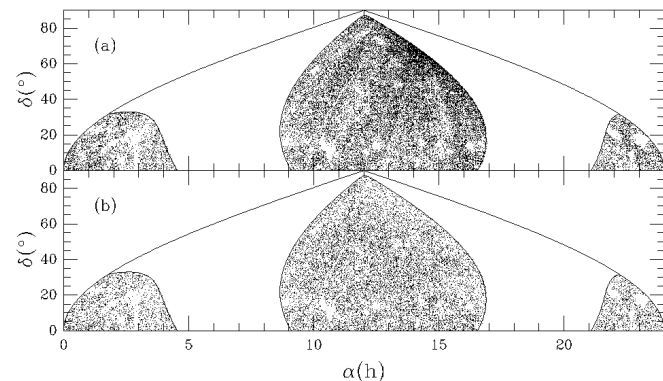

Fig. 2. Distribution over the sky of (a) the 29 321 ROSAT-FSC sources, (b) the 15 848 sources brighter than 0.02 counts s^{-1}.

2.2. Identification methodology

Our aim being to identify all bright extragalactic objects associated with a ROSAT-FSC source in the area defined above, we chose to make use of the Hamburg slitless survey of the northern sky which, in principle, allows us to determine the nature of every object brighter than O∼17.0. However this would require us to visually inspect all objects within a given radius around each of the 15 848 X-ray sources in the sample. This is obviously not feasible. We therefore decided to preselect all bright objects lying near the X-ray positions in the APS database, which is a catalogue of all objects visible on the Palomar Sky Survey plates, including magnitude, colour and classification as starlike or extended. But this could not be easily done as the APS was not directly available (when we started this work). The USNO catalogue is similar to the APS catalogue except that it does not classify the listed objects as starlike or extended; but it is available on CD-ROMs. It was therefore easy to select all bright USNO objects near the X-ray positions. We then sent the list of 3 776 selected objects to the University of Minnesota where a batch job was run to find their APS magnitude, colour and classification.

However, as very bright stars (O<12.0) are saturated on the DSS1 images and bright extended galaxies are poorly recognized by the automatic extraction procedures of both the USNO and APS databases, to find these objects we had to cross-correlate the X-ray catalogue with various catalogues of bright stars and galaxies. We ended up with 3 212 objects found in the APS database, 685 bright stars and 91 additional galaxies.

The APS classification as "star-like" or "extended" were then evaluated by visual screening of the DSS2 images. 2 719 APS objects were found to be "star-like" and 493 "extended". All 3 212 APS objects were subsequently classified using the digitized objective prism spectra of the Hamburg Quasar Survey.

Follow-up observations were started for the "extended" objects and additional galaxies having $O_{APS}<17.0$, showing the sample to be a mixture of galaxies containing 20% AGN.

The "star-like" objects were separated into several sub-samples according to their APS colour and magnitude. A sample of 144 high-probability AGN candidates was selected. Based on literature data and our own follow-up spectroscopy, 83 of them are now confirmed AGN.

2.3. The USNO and APS databases

To identify the X-ray sources with relatively bright optical counterparts we have cross-correlated our ROSAT sample with the USNO-A2.0 catalogue (Monet et al. 1996) from which we have extracted all objects in the magnitude range O=12.0-16.5 (4 420 441 i.e. 428 deg^{-2}). We have found 25 549 objects located within $2'$ of one of the 15 848 X-ray sources.
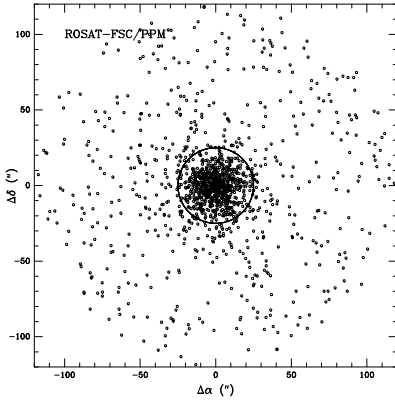
Fig. 3. Position differences for the coincidences between ROSAT-FSC X-ray sources and PPM stars within two arc minutes. The radius of the circle is $25''$.

As the USNO catalogue positions are rather poor for very bright objects, we have extracted the 1 306 PPM (Positions and Proper Motions) stars (Röser & Bastian 1991) located within $120''$ of a ROSAT position. The PPM star catalogue contains 181 731 stars north of declination $-2°.5$, brighter than about $m_{pg}=11.0$. Fig. 3 shows the distribution of the position differences between the ROSAT and PPM positions. The circle drawn on the figure has a radius of $25''$. The number of coincidences within this circle is 704 (with 19 X-ray sources being associated with two PPM stars), while the expected number of chance coincidences is 27. There are therefore 685 X-ray sources within $25''$ of at least one PPM star. We consider these 685 sources as identified; we ignored them in the following and we are left with 15 163 X-ray sources.
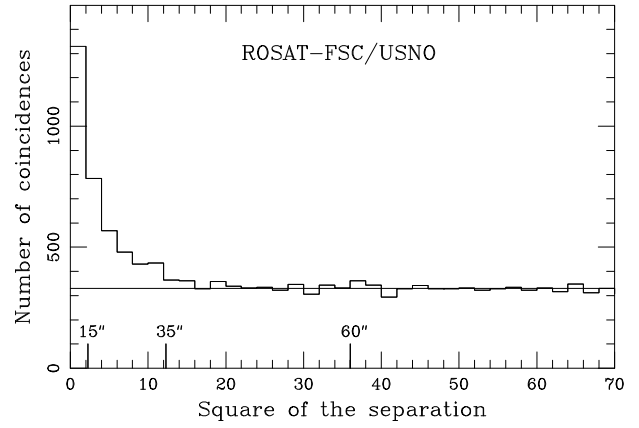
Fig. 4. Histogram of the square of the separation between the X-ray and USNO positions for the 25 549 associations in units of 100 square arcsec.

The histogram of the separation between the optical and X-ray positions (Fig. 4) shows that, for separations larger than $35''$, there is an overwhelming majority of chance coincidences. For smaller separations, the fraction of real associations rapidly increases. This empirically defined limit is a compromise to maximize the number of real associations and minimize the number of chance coincidences. It is not straightforward to determine the fraction of real associations having a separation larger than $35''$ and therefore lost by using this limit. For separations smaller than $35''$, there are 3 776 coincidences, half being expected by chance and half real. Including the PPM stars, about 17% of the X-ray FSC sources are therefore physically associated with a relatively bright object.

Zickgraf et al. (2003) found that the 90% error radius for the X-ray positions in the BSC is $21''$. This is significantly smaller than the value of $35''$ we used for the separation limit for real associations. This difference can probably be ascribed to the differences in count rates between the two samples.

In total there are 3 364 X-ray sources with at least one USNO object within $35''$: 2 985 with a single USNO object, 348 with two, 29 with three and 2 with four.

In the APS database (Cabanela et al. 2003), the objects are classified as starlike or resolved (galaxies). The photometric calibration for the starlike objects uses a magnitude-diameter relation derived from photoelectric calibrating sequences. The O magnitudes have a mean r.m.s. of 0.15-0.20 mag over the range 14-20 mag. These magnitudes are not as reliable for objects brighter than 12th mag because of the diffraction pattern. For objects brighter than 8th mag, photometry is not available. For galaxies, the integrated magnitudes are obtained from a density-to-intensity conversion. APS derived galaxy magnitudes show no systematic photometric errors and a typical r.m.s. scatter of 0.2 to 0.3 magnitudes. The O_{APS} and B magnitudes for stars are equal on aver-

age with a dispersion of 0.26 mag (Mickaelian et al. 1999).

In contrast, the USNO catalogue makes no distinction between starlike and extended objects. As a consequence, the magnitudes derived for galaxies are unreliable. The typical photometric error for starlike objects is about 0.31 mag r.m.s. (Mickaelian et al. 2001). Bright objects tend to saturate. The magnitudes reported for such objects are generally too high.

Figure 5 shows the comparison of the USNO and APS O magnitudes for starlike objects (left panel) and for galaxies (right panel). While the agreement between the two sets of magnitudes is reasonably good for starlike objects, it is very poor for galaxies.
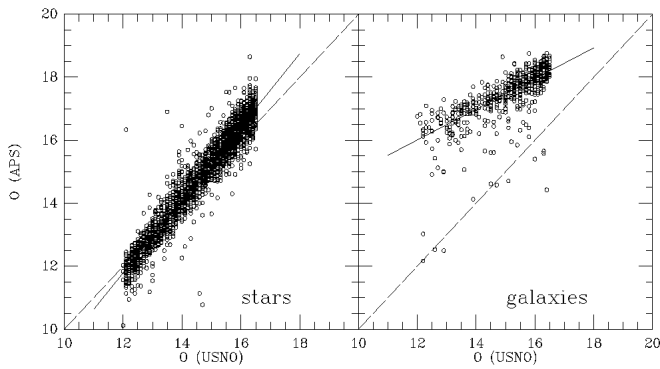

Fig. 6. Comparison of the USNO and APS O magnitudes with the NPM1 O magnitudes for 95 galaxies (filled squares) and 81 stars (open circles). The dotted lines have a slope of unity.

Fig. 5. Comparison of the USNO and APS O magnitudes for starlike objects (left panel) and for galaxies (right panel). The solid lines represent the best linear fits between the two sets of data; the dotted lines have a slope of unity.

Figure 6 shows the comparison of the USNO and APS O magnitudes with the NPM1 O magnitudes (Klemola et al. 1987) for 95 galaxies and 81 stars. The least square solutions for galaxies are:

$O_{NPM1G} = 0.47 \times O_{USNO} + 11.3$ ($\sigma = 0.54$ mag)
$O_{NPM1G} = 0.90 \times O_{APS} - 0.29$ ($\sigma = 0.50$ mag)

This confirms that, for galaxies, the APS magnitudes are more reliable than the USNO magnitudes. We therefore extracted from the APS database objects within $10''$ from the 3776 USNO objects, brighter than O=19.0. A number of these have no APS counterpart because the required plates were not available and 49 because there was no match. We checked these 49 USNO objects on the DSS2 images (Lasker et al 1996) and found that all of them, except one, have a starlike appearance. There are 3212 coincidences between USNO and APS objects (the 3212 sample), 2652 with starlike and 560 with extended objects.

As the APS classification based on DSS1 is not always correct, all 3212 images have been checked on the DSS2 plates. Of these, 2719 were classified as starlike and 493 as extended. Out of the 560 APS galaxies, 135 have been reclassified as starlike; 45 of them appear as binaries so that in the APS they appear as extended. On the other hand, 68 APS starlike objects have an extended image on the DSS2

2.4. The Hamburg database

All 3212 objects have been tentatively classified using the Hamburg slitless plates on the basis of a classification scheme introduced during the ROSAT-BSC identification program (Bade et al. 1998). The statistics of this classification is given in Table 1. Of the 493 objects classified as extended, based on direct images of the DSS2 plates, four could not be classified spectroscopically because of overlapping spectra. Based on their continua the 489 remaining objects were classified as "galaxy" (red continuum), "blue galaxy" (blue continuum) or "AGN" (prominent UV excess). Sixty one of the galaxies are member of a pair (23) or of a group (38). Among the starlike objects, 2181 were classified as stars due to absorption features in their spectra. The bright saturated objects ($O_{APS} < 12.0$) were also considered as stars. Moreover 383 starlike objects, too weak for the study of absorption features, were classified on the basis of their continuum: red (RED-WK), blue (BLUE-WK) and extremely blue (EBL-WK). These objects have typically $O_{APS} > 16.0$. Twenty two starlike objects were classified as QSOs due to the presence of a prominent UV excess and/or of emission lines. Fifty five objects could not be classified because of overlapping spectra and one more because its spectrum did not fit the classification scheme.

The HQS classifications have been checked with already known objects. In our sample there are 107 confirmed QSOs. Two could not be classified with the Hamburg material because of overlapping spectra. Seventeen have been classified as QSOs, one as an AGN, 56 as EBL-WK, 22 as BLUE-WK, two as RED-WK (J15563+0309, a low luminosity QSO with $M_B = -23.2$ and KUV 16355+4146 at z=0.765, with (O–E)=1.60) and

Table 1. Statistics of the HQS type of 3 212 optical associations with 2 982 ROSAT FSC sources.

HQS types	Number	%
AGN	6	0.2
Blue galaxy	215	6.7
Galaxy	268	8.3
QSO	22	0.7
EBL-WK	84	2.6
BLUE-WK	212	6.6
RED-WK	87	2.8
W-Dwarf	20	0.6
Star-BA	137	4.3
Star-FG	1325	41.3
Star-K	674	21.0
Star-M	25	0.8
Saturated	81	2.5
Overlap	55	1.7
Unidentified	1	0.0
Total	3212	100.0

seven as blue galaxies. These blue galaxies are in fact low luminosity QSOs ($M_B > -24.0$). On the other hand eleven EBL-WK objects have been shown to be stars, as well as 21 BLUE-WK and two RED-WK objects. Clearly the EBL-WK objects are good QSO candidates as well as the BLUE-WK, although to a lesser degree. When they are not QSOs, they usually turn out to be WDs or CVs.
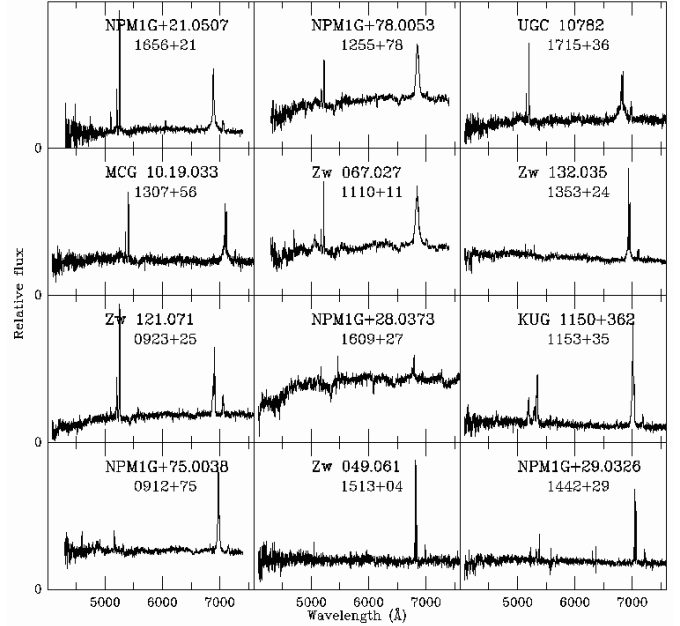
3. Galaxies

To find Seyfert galaxies we turned our attention to the 493 objects extended on the DSS2, found within $35''$ of an FSC source. If there were no real association, the number of coincidences within $15''$ would be 0.184 times the number of coincidences within $35''$ (the ratio of the respective areas). On the other hand, if all associations were real, Fig. 4 shows that almost all identifications would be located within $35''$ and about 50% within $15''$. In a sample in which the fraction of coincidences within $15''$ is x, the fraction y of true associations would be $y = (x - 0.184)/(0.5 - 0.184)$. 218 ($x=44$) of the 493 galaxies are within $15''$ of an X-ray source which shows that a large fraction of them ($y \sim 80\%$) are genuine associations.

As we have seen above, sixty eight of the objects found to be extended on the DSS2 were classified as starlike in the APS data base. Three of them (NGC 1085, IC 2439 and KUG 2323+85) were previously found to be bright galaxies and are included in Table 2. The 65 others are probably compact galaxies; 47 are classified as "blue galaxies" on the slitless HQS spectra (in fact, ten of them are already known to be Seyfert 1s or low luminosity QSOs).

As the spectroscopic observations took place before we had the opportunity to check the APS classification on the DSS2 images (which is a rather tedious procedure as it is done visually rather than automatically), these 65 objects were not included in our original list of galaxy candidates.

Of the 493 extended objects, 155 are brighter than $O_{APS} = 17.0$. Ninety four of them were classified as galaxies in the APS database. To these 94 galaxies we added 91 bright galaxies not appearing in the USNO or APS databases but found by cross-correlating the ROSAT FSC with catalogues of bright galaxies (NGC, UGC, NPM1G, Mark, Zw etc.). As the surface density in these catalogues is small, we accepted as identification all coincidences within $35''$. These 185 galaxy candidates are listed in Table 2. The redshift of 130 of them were known from the literature.

Fig. 7. Spectra of the six Seyfert 1, the three Seyfert 2 and three of the five starburst galaxies confirmed by our spectroscopic observations at BAO and OHP.

We have observed 34 of the galaxies without a previously known redshift at the BAO and OHP observatories. The BAO observations were made during the period March 3 to 10, 2002 with the 2.6-m telescope using the SCORPIO spectral camera attached to the prime focus. The combination of the detector, a 2063×2058 16×16 μm pixel Loral Lick3 CCD, with a 600 g mm^{-1} grism resulted in the spectral range 3900-7400 Å with a dispersion of 1.7 Å pixel^{-1}. The slit width was $1''.8$ (4.3 pixels) and was oriented EW. The spectral resolution was 5 Å FWHM. The exposure time was usually 45 min. The OHP observations were made between April 15 and 19, 2002 with the 1.93-m telescope and the spectrograph CARELEC (Lemaître et al. 1989) attached to the Cassegrain focus. The detector was a 2048×1024 13.5×13.5 μm pixel EEV CCD. The dispersion was 1.75 Å pixel^{-1} and the spectral range 4075-7715 Å. The slit width was $2''.0$, corresponding to 3.7 pixels, and the resolution was 5.7 Å FWHM. The exposure time was usually 20 min. We found 13 absorption line galaxies, five starburst galaxies, six Seyfert 1, three Seyfert

Table 2. List of the 185 galaxy candidates. Col. 1: right ascension, col. 2: declination, col. 3: separation between the ROSAT and USNO positions in arcsec, col. 4: X-ray count rate (count s^{-1}), col. 5: logarithm of the 0.1-2.4 keV X-ray luminosity (in erg s^{-1}), col. 6: magnitude O_{USNO}, col. 7: magnitude O_{APS}, col. 8: redshift, col. 9: classification (abs: galaxies with absorption lines only; em: emission line galaxies, but too weak to make a classification possible; C stands for Composite spectrum; S or S?: the object is certainly an AGN, but the lines are too weak for a more precise classification); col. 10: references: (1) BAO; (2) OHP, col. 11: name.

J2000 optical position									
h	m	s	°	′	″	sep(″)	c/r	L_X	O_{US}	O_{APS}	z		ref.	Name
0	14	7.46	10	34	13.3	5.3	0.036		15.0	16.89				
0	19	37.80	29	56	2.0	27.2	0.042	42.02		15.37	0.024			NGC 76
0	24	30.24	13	35	50.3	2.4	0.032		12.5	16.63				NPM1G+13.0013
0	46	29.20	8	25	59.6	18.9	0.023	42.18	15.5	16.32	0.039			UGC 482
0	54	45.23	16	26	17.2	9.2	0.038	42.37	13.6	16.56	0.038			MCG+03.03.008
0	54	48.64	28	52	1.1	26.7	0.024	41.74		15.66	0.023			UGC 555
0	57	48.89	30	21	8.8	7.3	0.043	41.67		13.14	0.016	Liner		NGC 315
1	16	14.83	31	2	1.8	34.2	0.021	41.42			0.017			NGC 452
1	20	38.97	29	41	43.9	9.4	0.031	41.85	16.0	15.40	0.023			IC 1672
1	30	35.46	19	36	31.0	4.2	0.034	42.43	13.7	16.35	0.043			UGC 1077
2	43	48.71	14	53	13.1	33.8	0.027	42.39		16.49	0.046			IC 1835
2	46	25.36	3	36	27.3	7.1	0.078	42.25	12.5	14.91	0.023			NGC 1085
2	51	12.98	13	11	31.3	16.1	0.031	41.92	13.8	16.34	0.025			UGC 2337B
2	58	51.14	6	22	25.9	5.4	0.026	42.35	13.5	16.88	0.045			LEDA 074274
7	50	8.28	55	23	2.9	18.6	0.032	41.70	12.6	15.43	0.019	abs	2	UGC 4035
8	1	55.04	62	32	15.0	6.0	0.034	42.88	14.0		0.072			
8	30	29.14	69	1	42.8	12.3	0.022	41.66	13.5		0.022			Zw 331.048
8	36	45.79	48	42	0.7	30.1	0.027		13.7	16.24				MCG+08.16.019
8	39	55.44	74	5	15.9	32.2	0.024		15.1					NPM1G+74.0038
8	55	38.01	78	13	25.3	5.0	0.024	40.41			0.005	Liner		NGC 2655
9	6	44.71	3	36	0.9	28.1	0.023		14.2					
9	8	38.35	32	35	34.0	15.9	0.033	41.44	12.4	15.79	0.014			IC 2439
9	11	37.50	60	2	15.0	22.9	0.026	40.45		12.12	0.005	S		NGC 2768
9	12	38.04	75	38	55.4	13.2	0.040	42.81	12.8		0.061	H II	1,2	NPM1G+75.0038
9	16	3.95	17	37	43.6	10.1	0.060	42.34		14.63	0.029			NGC 2795
9	16	50.01	20	11	54.6	19.8	0.021	41.85		15.04	0.028			NGC 2804
9	19	27.31	33	47	26.4	26.4	0.029	41.65	13.7	16.83	0.019			LEDA 139185
9	20	2.10	1	2	18.0	15.9	0.046	41.76		14.27	0.017			UGC 4956
9	23	25.93	22	19	1.0	20.3	0.081	42.50	13.9		0.030			UGC 4991b
9	23	24.36	22	18	47.3	5.4	0.081	42.60	13.4		0.034			UGC 4991a
9	23	29.19	25	46	9.6	13.4	0.021	42.35	12.5	15.73	0.050	S2	1,2	Zw 121.071
9	24	14.29	49	15	14.9	32.9	0.021	40.86		14.71	0.009			NGC 2856
9	25	28.30	23	36	31.6	1.5	0.035	42.21	12.2	16.12	0.033	em	1	Zw 121.086
9	25	42.55	11	25	55.3	14.6	0.034	41.25		14.31	0.011			NGC 2872
9	32	10.13	21	30	4.4	18.1	0.030	39.71			0.002	H II		NGC 2903
9	32	16.98	9	41	0.5	28.6	0.023		14.8	16.74				NPM1G+09.0188
9	38	12.30	7	43	39.8	19.9	0.033		13.8	16.84				Zw 035.017
9	38	32.90	17	1	52.0	17.9	0.040	42.13		16.00	0.028			NGC 2943
9	45	28.84	56	32	53.4	2.1	0.046	43.58	15.8	16.91	0.139	abs	1	
9	50	21.61	72	16	44.1	22.7	0.025	40.23			0.004	S1.9		NGC 2985
9	59	39.60	0	35	12.1	24.1	0.028	42.72	13.1	16.42	0.066			UGC 5370
10	1	57.80	55	40	47.1	4.2	0.049	40.53		12.23	0.004	S2		NGC 3079
10	6	7.45	47	15	45.4	22.0	0.036	41.98		15.09	0.025			NGC 3111
10	13	50.50	38	45	53.8	27.8	0.028	41.80		14.15	0.023			NGC 3158
10	27	49.91	36	33	34.7	24.4	0.037	42.34		16.02	0.037	S2		HS 1024+3648
10	32	33.34	65	2	0.9	33.2	0.023	40.55		14.42	0.006			NGC 3259
10	47	10.14	72	50	20.9	8.5	0.025	40.94			0.009			NGC 3348
10	51	29.91	46	44	41.5	24.1	0.026		13.3	16.00				NPM1G+47.0182
10	58	13.77	1	36	6.3	8.8	0.069	42.63	16.5		0.038	abs	1	UGC 6057c
10	58	13.04	1	36	24.3	29.9	0.069	42.65	15.1		0.039			UGC 6057b
11	0	5.35	14	50	26.5	28.4	0.026	40.45	15.9		0.005			NGC 3485
11	3	11.35	27	58	21.1	7.8	0.034	40.56	12.2	13.02	0.005	H II		NGC 3504
11	8	43.37	29	13	25.3	2.7	0.022	42.76	13.4	16.49	0.078	em	1,2	LEDA 094150
11	10	45.96	11	36	41.2	14.3	0.025	42.28	13.2	16.16	0.042	S1	1	Zw 067.027

Table 2. (continued)

h	m	s	°	′	″	sep(″)	c/r	L_X	O_{US}	O_{APS}	z		ref.	Name
11	15	2.23	4	5	7.4	13.4	0.024	42.19	13.4	16.48	0.039			Zw 039.090
11	24	43.64	38	45	46.3	22.1	0.051	41.03	12.9	12.50	0.007	H II		NGC 3665
11	25	45.33	24	8	24.5	28.9	0.029	41.86	12.7	15.12	0.024			Zw 126.051
11	28	2.16	78	59	40.4	16.3	0.046		14.7		0.000	H II		UGC 6456
11	34	6.64	25	33	34.8	18.9	0.029		12.8	16.55				MCG+04.27.068
11	39	14.88	17	8	37.2	4.2	0.037	41.85	13.1	16.23	0.021			UGC 6614
11	39	41.57	31	54	41.1	2.9	0.034	41.07	15.9		0.009	S1.8		NGC 3786
11	46	12.24	20	23	29.9	27.2	0.048	42.04	14.5	14.61	0.023	Liner		NGC 3884
11	47	22.16	35	1	7.5	25.9	0.044	42.87	14.4	16.60	0.063	S2		B2 1144+35B
11	49	59.31	21	20	1.1	9.2	0.026	41.88		15.32	0.026			NGC 3910
11	50	41.53	20	0	54.6	10.2	0.031	41.77		15.55	0.021			NGC 3919
11	53	26.26	35	56	53.8	15.3	0.023	42.66	12.3	16.27	0.068	S2	2	KUG 1150+362
11	59	52.16	55	32	5.4	30.6	0.024	42.83	13.7	16.96	0.081			PGC 2505536
12	4	6.25	20	14	6.2	25.5	0.028	41.72	12.9	14.99	0.021			NGC 4065
12	4	43.34	31	10	38.2	16.7	0.025	41.83		15.11	0.025	S1.9		UGC 7064
12	5	49.83	35	10	46.4	11.9	0.190	43.38	12.7	16.74	0.054	S1		Mark 646
12	8	5.56	25	14	14.1	16.0	0.034	41.89		15.32	0.023			UGC 7115
12	10	33.61	30	24	5.9	21.4	0.045	39.29		13.71	0.001	C		NGC 4150
12	14	18.10	29	31	4.5	5.0	0.021	42.57		16.96	0.064	S2		WAS 49b
12	14	48.65	59	54	22.5	23.3	0.028	42.64	14.6	15.61	0.060			NGC 4199a
12	14	51.71	59	54	30.5	4.5	0.028	42.65	16.3		0.061	abs	1	NGC 4199b
12	15	5.34	76	14	10.0	34.4	0.031	40.68			0.006			UGC 7265
12	16	0.00	12	41	1.4	5.4	0.033	42.78		16.60	0.065	S1.9		Mark 764
12	19	51.66	28	25	21.7	12.6	0.046	42.13	13.8	16.27	0.026			Zw 158.075
12	20	6.86	29	16	50.5	11.4	0.037	39.80	12.6	12.53	0.002	Liner		NGC 4278
12	22	54.89	15	49	20.7	15.6	0.042	40.65		11.30	0.005	C		NGC 4321
12	23	39.10	7	3	14.0	24.6	0.030	40.06		14.80	0.003			NGC 4342
12	23	42.85	58	14	45.9	10.3	0.037	41.55	14.5	16.93	0.015	S?		SBS 1221+585
12	26	28.02	9	1	23.0	26.7	0.029	41.86	14.7	14.58	0.024	Liner		NGC 4410
12	26	26.98	31	13	22.6	4.4	0.033	39.75	12.2	12.17	0.002	C		NGC 4414
12	28	29.49	17	5	6.0	9.8	0.039	40.91		12.21	0.007	Liner		NGC 4450
12	34	3.10	7	41	59.0	24.2	0.032	39.14		11.85	0.001	H II		NGC 4526
12	34	46.81	47	45	32.4	34.2	0.043	42.25		16.12	0.031			MCG+08.23.061
12	48	58.34	40	35	56.8	14.5	0.039	41.58	15.2	15.95	0.015			IC 3808
12	50	26.60	25	30	5.8	8.3	0.028	40.28		11.04	0.004	S2		NGC 4725
12	55	7.78	78	37	14.9	4.1	0.029	42.36	12.9		0.043	S1	1	NPM1G+78.0053
12	56	43.76	21	40	51.9	7.2	0.041	39.25		10.36	0.001	S		NGC 4826
12	59	39.35	38	48	56.3	16.0	0.022	42.01	13.2	16.23	0.033			IC 4003
13	0	39.13	2	30	5.3	22.4	0.027	40.02		12.98	0.003	H II		NGC 4900
13	4	40.89	43	18	35.0	20.1	0.031		14.0	16.86				NPM1G+43.0235
13	4	57.99	43	33	10.9	25.2	0.052		13.1	16.06				MCG+07.27.026
13	7	3.03	56	31	59.2	5.5	0.044	43.08	12.4	16.40	0.080	S1	1,2	MCG+10.19.033
13	20	28.94	31	21	6.9	19.8	0.029	42.42	12.8	16.53	0.046			Zw 160.204
13	29	58.73	47	16	4.5	29.1	0.046	39.90		11.51	0.002	Liner		NGC 5195
13	32	48.62	41	52	18.9	12.3	0.038	42.07		14.08	0.027			NGC 5214
13	38	17.27	48	16	32.0	18.4	0.043	42.16		15.05	0.028	S2		Mark 266SW
13	42	8.34	35	39	15.2	15.3	0.021	40.16		13.06	0.004	S1.9		NGC 5273
13	44	1.90	25	56	27.8	28.5	0.026		12.8	17.00				
13	51	4.24	19	26	8.2	3.7	0.048	42.90	13.5	16.95	0.062	em	1,2	
13	51	42.19	55	59	43.2	29.3	0.022		15.1	16.68				TEX 1349+562
13	53	9.75	24	22	37.4	6.6	0.027	42.26	13.5	16.85	0.056	S1	1,2	Zw 132.035
13	53	26.69	40	16	58.9	7.7	0.048	41.12			0.008	Liner		NGC 5353
13	53	43.82	33	13	20.3	28.2	0.024	42.43	14.5	15.61	0.051			MCG +06.31.015
13	53	55.94	21	59	54.9	24.1	0.042		12.9	16.86				
13	58	19.76	7	13	15.2	27.4	0.044	42.07	15.7		0.025			Zw 046.025
14	12	36.95	39	18	53.8	21.2	0.034	41.96	16.4	15.27	0.025	S1.9		NGC 5515
14	13	23.13	24	31	56.8	24.3	0.024	42.44	12.2	16.34	0.052	abs	2	Zw 133.012
14	18	9.20	7	33	52.0	24.3	0.042	42.02		14.97	0.024			NGC 5546

Table 2. (continued)

J2000 optical position						sep(")	c/r	L_X	O_{US}	O_{APS}	z		ref.	Name
h	m	s	°	'	"									
14	22	55.37	32	51	2.7	2.0	0.028	42.14		15.28	0.034	S1.8		UGC 9214
14	26	2.32	8	6	40.5	34.6	0.024	41.84		16.98	0.026			Zw 047.039
14	26	18.64	26	14	52.3	13.8	0.027	42.02	16.3	15.58	0.030			IC 4423
14	28	23.06	78	53	8.2	0.2	0.047	42.03	12.1		0.023			IC 4470
14	29	40.64	0	21	59.2	13.8	0.025	42.51	14.8	16.92	0.055	abs	1	Zw 019.045
14	29	48.51	53	57	54.3	25.6	0.025	42.30	13.2	16.19	0.043			IC 1027
14	42	39.65	29	20	48.2	7.5	0.028	42.82	13.5	17.00	0.074	H II	1,2	NPM1G+29.0326
14	50	51.40	5	6	52.0	25.9	0.025	41.92		15.29	0.028	S2		NGC 5765B
14	50	55.42	27	34	42.1	13.1	0.032	42.09		15.89	0.030			IC 4514
14	51	14.39	30	41	32.2	33.9	0.044		12.5	16.28				Zw 164.036
14	55	28.21	32	50	24.0	30.3	0.026		14.1	16.21				MCG+06.33.009
15	4	15.88	28	29	47.5	32.7	0.127	43.26		15.66	0.058			MCG+05.36.002
15	5	56.60	3	42	26.0	15.6	0.027	42.18		16.00	0.036	S1.8		Mark 1392
15	9	20.51	7	38	19.4	28.5	0.044	43.05	16.0	16.94	0.077	abs	2	
15	13	40.25	4	4	17.2	24.9	0.025	42.21	13.3	16.96	0.039	H II	2	Zw 049.061
15	20	29.00	44	58	15.3	11.5	0.046	42.89	13.9	16.86	0.063	abs	1	
15	21	20.58	30	40	15.3	15.0	0.139	43.57	14.0	16.93	0.079	abs	2	Zw 165.041
15	23	59.90	31	12	40.2	31.4	0.032	42.97		16.71	0.074			MCG+05.36.026
15	25	8.75	12	52	57.5	24.6	0.039	41.95	12.5	16.30	0.023			Zw 077.123
15	29	14.68	52	51	50.1	12.9	0.029	42.80	13.1	16.66	0.071	abs	1	UGC 9868
15	32	32.02	4	40	51.4	13.8	0.048	42.50		15.75	0.039			UGC 9886
15	32	57.19	0	26	36.1	11.4	0.044	42.41	15.8	16.11	0.037			Zw 022.010
15	33	17.73	82	13	46.2	11.3	0.036	41.87	12.9		0.022			UGC 9950
15	35	54.26	14	31	2.7	34.6	0.049	41.92		15.70	0.020	S2		Akn 479
15	38	10.00	57	36	12.0	12.1	0.034	42.90		16.20	0.074	S1		MCG+10.22.028
15	39	2.65	31	45	34.3	25.4	0.031	40.81		15.31	0.007			NGC 5974
15	47	48.93	37	1	36.0	19.9	0.040	43.01	15.1	16.60	0.077	em	2	NPM1G+37.0489
15	52	12.04	34	5	35.4	24.0	0.024	42.43	14.7		0.051	abs	2	NPM1G+34.0353
15	56	41.39	20	10	16.4	33.0	0.027		12.8	16.66				
16	4	55.53	28	9	56.9	21.8	0.047	43.08	12.1	16.54	0.077			Zw 167.022
16	5	29.18	16	25	8.8	28.3	0.041	42.53			0.044			UGC 10187B
16	5	35.57	44	12	22.0	16.9	0.056	42.65	13.5	16.33	0.043			MCG+07.33.038
16	5	36.83	17	48	8.1	32.0	0.025	42.09		16.32	0.034	H II		Mark 298
16	7	24.03	85	1	49.3	2.7	0.042	43.78	16.5		0.183	S1		S5 1616+85
16	7	35.36	13	56	37.6	28.9	0.026	42.11	13.1	16.21	0.034			NGC 6066
16	9	5.53	27	53	34.0	10.2	0.041	42.23	12.5	16.84	0.031	S2	1,2	NPM1G+28.0373
16	9	35.18	63	58	1.2	8.2	0.047	42.75	14.0	16.82	0.053	em	1,2	NPM1G+64.0143
16	11	11.40	61	16	4.5	13.2	0.030	42.09		14.95	0.031			NGC 6095
16	11	13.89	36	58	24.3	27.6	0.031	42.79	12.5	16.95	0.068	abs	2	KUG 1609+371A
16	12	33.72	29	29	39.1	15.5	0.043	42.28	13.6	15.07	0.032			NGC 6086
16	24	37.00	19	30	24.3	11.2	0.026	42.16			0.036			Zw 109.013
16	27	42.60	39	22	38.5	13.7	0.023	41.92	16.1		0.029			PGC 058195
16	29	44.90	40	48	41.8	6.2	0.039	42.15		14.31	0.029			NGC 6173
16	29	52.80	24	26	38.1	6.3	0.041	42.40	12.2	16.30	0.038	S1.9		Mark 883
16	32	58.03	11	43	23.8	27.5	0.038	42.71	16.3	15.65	0.056			Zw 080.046
16	33	48.87	35	53	18.8	33.3	0.022	42.13		16.57	0.038			KUG 1632+359
16	36	57.72	55	46	58.2	8.6	0.038	42.11	13.5	16.92	0.028	S?	1,2	
16	37	20.55	41	11	20.1	16.3	0.038	42.22	13.0	16.74	0.032	abs	2	NPM1G+41.0441
16	39	4.72	8	21	30.9	11.2	0.035	42.48	13.2	16.88	0.045	em	2	NPM1G+08.0448
16	42	56.33	19	15	15.5	10.6	0.042	42.32	13.0	16.25	0.034			IC 1224
16	43	4.22	61	34	43.3	22.7	0.032	41.70	13.9	14.13	0.019			NGC 6223
16	56	1.58	21	12	42.0	10.4	0.028	42.46	15.4	16.99	0.049	S1	1	NPM1G+21.0507
16	57	45.01	68	30	53.1	13.9	0.045	42.42	13.1	15.88	0.037			NGC 6289
17	0	27.21	51	59	11.6	14.3	0.044	42.64	12.7	16.87	0.048	S1		NPM1G+52.0273
17	3	47.89	34	43	39.2	20.0	0.023		12.2					
17	12	36.58	38	1	13.3	25.4	0.040	42.37		15.40	0.037			IC 1245
17	15	58.85	36	23	23.1	15.2	0.048	43.18	13.6	16.13	0.086	S1	2	UGC 10782
17	23	22.08	32	49	55.2	16.7	0.022	42.63	13.2	16.55	0.067	H II	2	

Table 2. (end)

	J2000 optical position													
h	m	s	°	′	″	sep(″)	c/r	L_X	O_{US}	O_{APS}	z		ref.	Name
17	37	56.34	41	38	32.0	19.9	0.023	42.68	15.1	16.39	0.070	H II	2	IRAS F17363+4140
17	38	11.38	58	42	55.3	21.7	0.034	42.09		15.85	0.029	S1		NGC 6418
22	21	47.39	2	54	36.2	24.5	0.028		13.2	16.72				
22	28	29.51	16	46	59.6	11.6	0.034	42.23	12.9	15.01	0.034			NGC 7291
22	32	30.68	8	12	33.0	18.2	0.034	41.96	12.5	16.08	0.025	S1		Akn 557
22	35	40.82	1	29	5.9	26.2	0.293	43.64	14.3	16.63	0.059			LEDA 087323
22	41	34.22	4	53	10.7	34.3	0.047	42.97		16.90	0.068	S?		NPM1G+04.0574
22	49	54.69	11	36	30.1	23.7	0.054	42.19		14.35	0.026			NGC 7385
22	58	1.97	13	8	4.4	10.7	0.021	41.75		15.08	0.025			NGC 7432
23	13	58.36	3	42	54.4	5.6	0.031	42.62	13.0	16.42	0.056			Zw 380.012
23	20	42.29	8	13	2.5	7.2	0.035	41.26			0.011	Liner		NGC 7626
23	25	51.50	8	47	11.2	6.6	0.025		14.3	16.46				KUG 2323+085
23	31	50.20	25	32	40.0	6.7	0.038		13.3	16.59				KUG 2329+252
23	36	14.10	2	9	18.6	3.5	0.021	40.86			0.009	H II		NGC 7714
23	56	1.96	7	31	23.4	3.1	0.049	42.53	13.6	16.84	0.040	S1		Mark 541

2 and seven unclassifiable weak emission line galaxies. Fig. 7 shows the spectra of the Seyfert 1 and 2 galaxies and of three starburst galaxies.

In total the redshift of 164 of the galaxies is known. We have computed their 0.1-2.4 keV X-ray luminosity. Sixty-three are smaller than 10^{42} erg s^{-1} and forty-five, greater than $10^{42.5}$ erg s^{-1}. As there are probably no starburst galaxies having an 0.1-2.4 keV X-ray luminosity substantially higher than 10^{42} erg s^{-1} (Moran et al. 1996; Condon et al. 1998), most of the 45 high X-ray luminosity galaxies must be AGN. Among the 16 which have been classified, four are starbursts and 12 AGN. The 63 low X-ray luminosity galaxies could possibly be absorbed Seyfert 2s, low-luminosity AGN as well as starbursts, or elliptical galaxies with hot gas (Hornschemeier et al. 2001; 2003; Comastri et al. 2003; Severgnini et al. 2003). Several of our low X-ray luminosity sources have been classified as Liners, Seyfert 2s, Seyfert 1.9 or 1.8.

4. QSOs

Figure 8 (a) shows the APS O–E colour index *vs* the O magnitude for the 2 652 starlike objects in the 3 212 sample. Fig. 8 (b) is the same for objects within 15″ of a ROSAT-FSC source. These figures were divided into four zones.

Objects brighter than O_{APS}=13.5 (zone I) are most probably bright stars. Indeed among the 576 objects in this zone, 84 could not be classified on the Hamburg slit-less spectra because of saturation or overlap, but all others are stars (25 BA, 416 FG and 51 K). Objects located above the diagonal line (zone II) are very red and are likely to be late-type stars. Fig. 8 (c) shows that indeed K and M stars are mostly located in this zone. Among the 709 objects in this zone, 13 are affected by overlapping or saturation, 685 are stars (including 437 K stars); 11 were too weak to be classified.
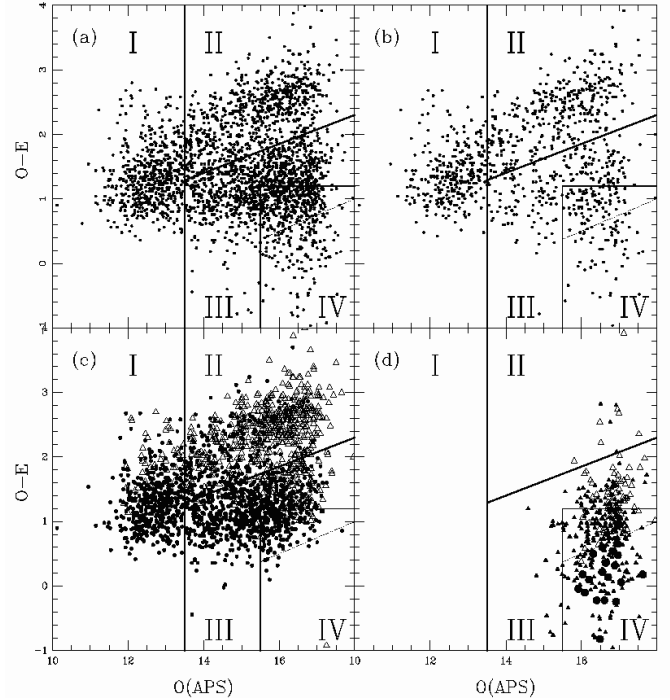

Fig. 8. (a) APS O–E colour indices *vs* O magnitudes for all starlike candidate identifications within 35″; (b) the same for coincidences within 15″; (c) the same for the A to G stars (filled circles) and the K and M stars (open triangles) as classified according to the Hamburg scheme; (d) the same for the BLUE-WK and EBL-WK objects (filled triangles), the RED-WK objects (open triangles) and the QSOs (filled circles).

We cross-correlated the FSC with the current version of the Véron-Cetty & Véron (2001) AGN catalogue. We found 76 coincidences within 35″ with a previously known AGN brighter than O_{USNO}=16.5 (they are listed in Table 3); 68 have magnitude and colour in the APS database.

Table 3. List of the 76 known AGN brighter than $O_{USNO}=16.5$, located within $35''$ of a ROSAT-FSC source. Col. 1: right ascension, col. 2: declination, col. 3: separation between the ROSAT and USNO positions in arcsec, col. 4: X-ray count rate (count s^{-1}), col. 5: magnitude O_{USNO}, col. 6: magnitude O_{APS}, col. 7: APS O–E colour, col. 8: redshift, col. 9: absolute magnitude computed by using the O_{USNO} magnitude ($H_o=50$ km s^{-1} Mpc^{-1}), col. 10: classification, col. 11: name.

	J2000 USNO position												
h	m	s	°	′	″	″	c/r	O_{US}	O_{APS}	O–E	z	M_{abs}		Name
0	6	23.08	12	35	53.2	20.8	0.030	15.8	16.26	0.36	0.98	−28.4	Q	RGB J0006+125
0	24	44.10	0	32	21.4	9.7	0.047	16.2	16.92	0.58	0.404	−25.8	Q	PB 5932
0	36	12.50	5	49	52.0	9.1	0.064	16.3	16.88	0.28	0.41	−25.7	Q	HS 0033+0533
0	52	5.57	0	35	38.4	28.6	0.024	16.3	16.80	1.04	0.399	−25.7	Q	Q 0049+0019A
0	57	9.93	14	46	10.4	26.7	0.246	15.9	16.11	1.12	0.171	−24.0	Q	PHL 909
1	20	17.29	21	33	46.6	25.0	0.023	15.5	15.80	0.54	1.500	−29.7	Q	PG 0117+213
1	39	55.80	6	19	22.5	8.4	0.031	15.7	16.55	0.60	0.396	−26.5	Q	PHL 1092
1	40	35.02	23	44	51.1	25.1	0.029	16.1	16.64	0.98	0.32	−25.4	Q	HS 0137+2329
1	41	59.60	6	12	5.5	2.7	0.049	16.3	16.27	0.56	0.345	−27.2	Q	PHL 1106
3	18	25.57	15	59	56.7	11.2	0.033	16.3	16.58	0.02	0.515	−25.9	Q	US 3828
3	39	9.60	3	45	52.5	23.7	0.038	16.4	17.55	0.44	0.199	−24.0	Q	RXS J03391+0346
4	24	46.85	0	36	6.4	7.4	0.052	16.1	16.75	1.26			BL	PKS 0422+00
8	15	59.21	41	44	57.1	17.9	0.021	15.8	15.97	0.32	1.28	−29.3	Q	KUV 08126+4154
8	22	36.88	54	18	36.4	33.7	0.042	16.3	16.65	1.12	0.086	−22.3	S1	SBS 0818+544
8	43	49.78	26	19	11.1	19.4	0.068	16.4	17.23	0.20	0.258	−24.7	Q	HS 0840+2630
8	59	24.35	46	37	17.3	22.3	0.047	16.5	16.89	0.74	0.923	−27.5	Q	US 2068
9	0	47.30	74	44	26.3	16.6	0.045	16.1			0.77	−27.4	Q	HS 0855+7456
9	19	57.63	51	6	9.1	17.1	0.039	15.8	16.35	−0.80	0.553	−27.0	Q	SBS 0916+513
9	25	14.35	54	44	27.2	10.4	0.048	15.9	16.66	−0.12	0.476	−26.3	Q	SBS 0921+549
9	29	9.82	46	44	24.1	15.9	0.025	15.6	15.66	0.18	0.240	−25.3	Q	US 645
9	36	25.45	39	49	33.7	24.8	0.033	16.1	16.81	0.82	1.25	−28.7	Q	KUV 09333+4003
9	37	1.93	34	25	0.0	12.7	0.031	16.0	16.55	0.22	0.908	−28.1	Q	Ton 1078
9	41	33.72	59	48	11.3	13.2	0.045	16.3	16.70	0.36	0.966	−27.9	Q	SBS 0938+600
9	56	49.89	25	15	16.0	8.0	0.048	16.2	16.92	0.84	0.712	−27.2	Q	OK 290
10	4	20.10	5	13	0.6	22.1	0.021	16.2	16.55	0.26	0.161	−23.8	Q	PG 1001+054
10	13	30.20	53	15	59.6	6.7	0.025	16.2	16.64	0.36	1.495	−29.1	Q	SBS 1010+535
10	15	57.04	1	9	13.7	16.1	0.082	16.3	16.97	0.94	0.779	−27.2	Q	Q 1013+0124
10	33	59.50	35	55	9.0	14.9	0.046	16.3	16.76	0.92	0.169	−23.8	Q	CSO 275
10	43	55.52	56	27	57.0	18.6	0.028	16.3	16.81	−0.40	1.951	−29.6	Q	SBS 1040+567
11	17	6.41	44	13	33.8	8.1	0.023	14.8	15.06	0.40	0.144	−24.9	Q	PG 1114+445
11	30	4.76	41	16	19.5	23.2	0.035	15.7	16.20	0.10	1.530	−29.5	Q	KUV 11274+4133
11	33	35.40	9	39	1.8	24.6	0.029	16.4	17.05	0.06	0.379	−25.5	Q	RX J11335+0939
11	43	47.71	11	28	48.1	20.6	0.046	15.5	16.38	0.80	0.118	−23.8	Q	RX J11437+1128
11	52	51.90	33	7	18.8	2.7	0.033	16.1	16.30	0.40	1.389	−28.8	Q	CSO 373
11	55	7.62	52	1	29.4	6.4	0.036	16.4	16.46	1.08	0.156	−23.5	Q	SBS 1152+523
11	59	6.78	53	6	43.5	6.1	0.043	16.5	17.19	0.36	0.482	−25.9	Q	MS 11565+5323
12	7	4.53	38	40	24.6	3.7	0.045	16.3	16.64	0.00	0.572	−26.4	Q	RXS J12070+3840
12	17	40.83	49	31	17.9	1.1	0.049	16.5	17.62	0.18	0.730	−26.6	Q	SBS 1215+497
12	22	10.01	27	19	2.3	6.4	0.046	15.9	16.90	0.52	0.442	−26.3	Q	RXS J12221+2719
12	23	0.23	55	40	0.3	9.4	0.057	16.5	17.48	0.48	0.905	−27.5	Q	SBS 1220+559
12	28	24.97	31	28	37.7	24.8	0.024	15.6	16.28	0.28	2.219	−30.4	Q	B2 1225+31
12	30	50.04	1	15	22.6	6.4	0.041	14.4	14.81	0.16	0.117	−24.8	Q	RX J12308+0115
12	33	26.05	45	12	23.1	11.2	0.032	16.5	16.91	−0.24	1.958	−29.4	Q	HS 1231+4528
12	44	10.82	17	21	4.5	16.3	0.027	15.7	16.58	0.74	1.283	−28.8	Q	PG 1241+176
13	6	5.72	80	8	20.5	10.9	0.035	16.3			1.183	−28.3	Q	S5 1305+80
13	13	21.39	78	21	53.9	11.9	0.026	15.6			2.00	−30.3	Q	HS 1312+7837
13	19	56.24	27	28	8.4	23.4	0.031	15.5	16.54	0.22	1.014	−28.7	Q	CSO 873
13	41	0.81	41	23	14.2	17.0	0.022	16.4	16.36	−0.02	1.204	−28.3	Q	PG 1338+416
13	47	19.40	59	2	32.5	10.3	0.025	16.2	16.48	0.22	0.768	−27.3	Q	SBS 1345+592
13	47	37.45	30	12	52.4	20.5	0.035	15.7	16.12	0.68	0.118	−23.6	Q	Q J1347+3012
13	51	28.30	1	3	38.5	17.5	0.040	16.5	17.35	0.58	1.086	−27.9	Q	Q 1348+0118
14	2	44.52	15	59	56.2	1.9	0.031	16.3	16.66	1.56	0.245	−24.5	BL	MC 1400+162
14	27	35.60	26	32	14.5	26.8	0.040	15.4	15.18	−0.72	0.366	−26.6	Q	PG 1425+267
14	36	45.79	63	36	37.6	32.1	0.038	15.7	16.61	−0.22	2.066	−30.4	Q	S4 1435+63
14	50	26.68	58	39	44.7	9.9	0.046	15.8	16.13	1.14	0.210	−23.8	Q	Mark 830
14	51	53.63	72	14	46.8	5.8	0.027	16.3			0.75	−27.1	Q	HS 1451+7227

Table 3. (end)

| | J2000 USNO position | | | | | | | | | | | | | |
h	m	s	°	′	″	″	c/r	O_{US}	O_{APS}	O–E	z	M_{abs}		Name
15	27	28.64	65	48	10.3	14.0	0.046	16.2	16.77	0.56	0.345	−25.5	Q	FBS 1526+659
15	50	43.65	11	20	47.4	23.7	0.040	16.3	16.33	0.14	0.436	−25.9	Q	MC 1548+114
15	51	58.16	58	6	44.7	4.5	0.036	16.2	16.74	1.14	1.320	−28.7	Q	SBS 1550+582
16	19	40.54	25	43	23.3	13.1	0.035	16.4	16.62	1.36	0.268	−24.7	Q	RX J16196+2543
16	23	19.93	41	17	2.7	26.3	0.030	16.5	16.88	0.32	1.618	−28.9	Q	KUV 16217+4124
16	26	37.28	58	9	17.2	6.0	0.044	16.2			0.751	−27.2	Q	SBS 1625+582
16	28	25.70	8	33	0.1	10.1	0.031	16.4	17.22	0.32	0.44	−25.8	Q	HS 1626+0839
16	31	43.83	52	53	43.8	5.7	0.048	16.5	16.81	0.44	0.352	−25.2	Q	SBS 1630+530
16	32	1.11	37	37	50.0	14.5	0.034	16.0	16.60	0.54	1.478	−29.4	Q	PG 1630+377
16	32	34.68	73	59	43.0	3.2	0.030	16.1			0.208	−24.4	Q	RXS J16325+7359
16	34	29.01	70	31	32.3	1.2	0.049	14.9			1.337	−30.1	Q	PG 1634+706
16	37	7.53	41	40	26.9	17.0	0.028	16.2	16.28	1.60	0.765	−27.3	Q	KUV 16355+4146
17	1	0.62	64	12	9.3	19.0	0.035	15.9	16.03	0.18	2.736	−31.2	Q	HS 1700+6416
17	4	41.39	60	44	30.5	8.4	0.042	15.6	15.86	0.76	0.371	−26.3	Q	3C 351.0
17	6	48.06	32	14	22.9	17.0	0.029	16.2	16.94	0.66	1.070	−28.2	Q	RGB J1706+322
17	19	34.18	25	10	58.6	16.9	0.039	16.4	16.87	1.34	0.579	−26.4	Q	RX J17195+2510
22	53	7.37	19	42	34.7	21.5	0.039	16.4	16.75	0.92	0.284	−24.9	Q	HS 2250+1926
23	7	45.62	19	1	20.8	11.6	0.033	16.4	17.13	0.98	0.313	−25.0	Q	PKS 2305+18
23	11	59.50	9	26	1.4	7.4	0.048	16.3	17.51	0.16	0.479	−26.1	Q	RX J23119+0925
23	50	10.07	8	12	55.3	16.6	0.025	16.4	18.19		1.70	−29.1	Q	HS 2347+0756
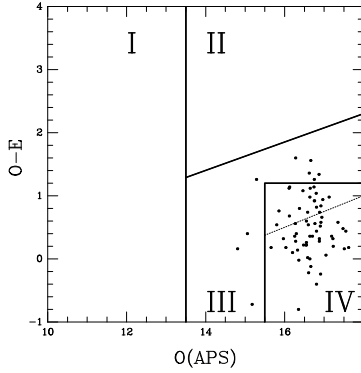
Fig. 9. APS O–E colour indices *vs* O magnitudes for 68 confirmed QSOs.

Fig. 10. Position differences between the ROSAT-FSC X-ray sources and APS starlike objects located in each of the four zones previously defined. The circles have a radius of 15″ and 35″, respectively.

Fig. 9 is a plot of the APS O–E colour index *vs* the O magnitude for these 68 AGN; 87% (59/68) are located in zone IV defined by $O_{APS}>15.5$ and O–E<1.2. With this limit on O–E, we exclude red QSOs; this is unavoidable because of the very large number of stars with O–E>1.2. These objects can be recovered by examination of the slit-less spectra. Figs. 8 (d) and 9 show that the distributions of the representative points of the EBL-WK and BLUE-WK objects on the one hand and of that of QSOs on the other hand are quite similar.

Figure 10 shows the differences between the X-ray and optical positions for the starlike objects in the 3 212 sample in each of the four zones defined above. In the first two zones there is an obvious concentration towards the centre showing that most of the coincidences are genuine associations. In contrast the distribution of the points in zone III is quite uniform suggesting that most of these coincidences are due to chance.

In zone III, the observed fraction of coincidences within 15″ is $x=0.20$, suggesting that there are indeed very few true associations ($y=0.05$). On the other hand, in zone I

and II, we found x=0.47 and 0.45 respectively showing that basically all objects (90 and 84% respectively) are real associations.

For the 212 starlike objects classified as BLUE-WK on the Hamburg slitless spectra, we found x=0.24, so the fraction of true coincidences is about 18%, while for the 84 EBL-WK objects, x=0.51 and, within the statistical uncertainties, all are genuine associations.

Out of the 2652 starlike objects, zone IV contains 476 coincidences within 35″ and 136 (x=0.28) within 15″ of an X-ray source, implying that y=0.32; therefore 153 of these coincidences are likely to be genuine associations, 76 being located within 15″. They could be blue stars (WD, CV, sd), or more probably QSOs. We have divided zone IV in two subregions (see the dotted line on Fig. 8). In the upper region (IVb), only 23% of the coincidences are within 15″ and therefore a small fraction of the 332 coincidences are genuine. In the lower region (IVa) containing the bluest objects, 41% of the coincidences are located within 15″ from the X-ray source, suggesting that ∼70% of the 144 objects located in this zone are real identifications. Among them are 41 known QSOs. The 103 other candidates, of which seven are known stars, are listed in Table 4. We have spectroscopically observed 91 of them. The observations were carried out during three observing runs (May and August 2002 and May 2003) with the 2.1-m telescope of the Guillermo Haro Astrophysical Observatory (OAGH) located in Cananea (Sonora, Mexico), operated by INAOE, and one run (September 2003) with the OHP 1.93-m telescope and the same instrument setting as for the observations of the galaxies (see section 3). The 2.1-m telescope was equipped with the LFOSC focal reducer (Zickgraf et al. 1997). The slit mask and the lower dispersion grism were used, giving a wavelength coverage from 4200 Å to 9000 Å and a dispersion of 8.2 Å pix^{-1}. We found 49 stars (including a CV the spectrum of which is shown in Fig. 11), 38 QSOs, 1 Seyfert 1, two NLS1s, one BL Lac object (their spectra are displayed in Figs. 12, 13 and 14). Five candidates have not yet been observed.

Altogether, there are, in region IVa, 83 confirmed AGN in a total of 139 spectroscopically observed starlike objects (60%).

But only 60% (41/68) of all previously known AGN with APS colour fall in zone IVa showing the limits of the efficiency of the procedure we have adopted. The others are located in zone IVb, or not far from it, in a region where chance coincidences between stars and X-ray sources become non negligible. Here the Hamburg slitless spectra may turn out to be most useful in separating AGN from stars.

5. Discussion

5.1. Identification procedure

We have seen that the galaxies found within 35″ of a ROSAT source have a high probability of being genuine
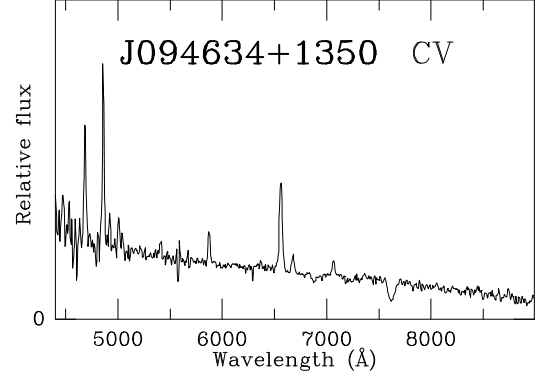

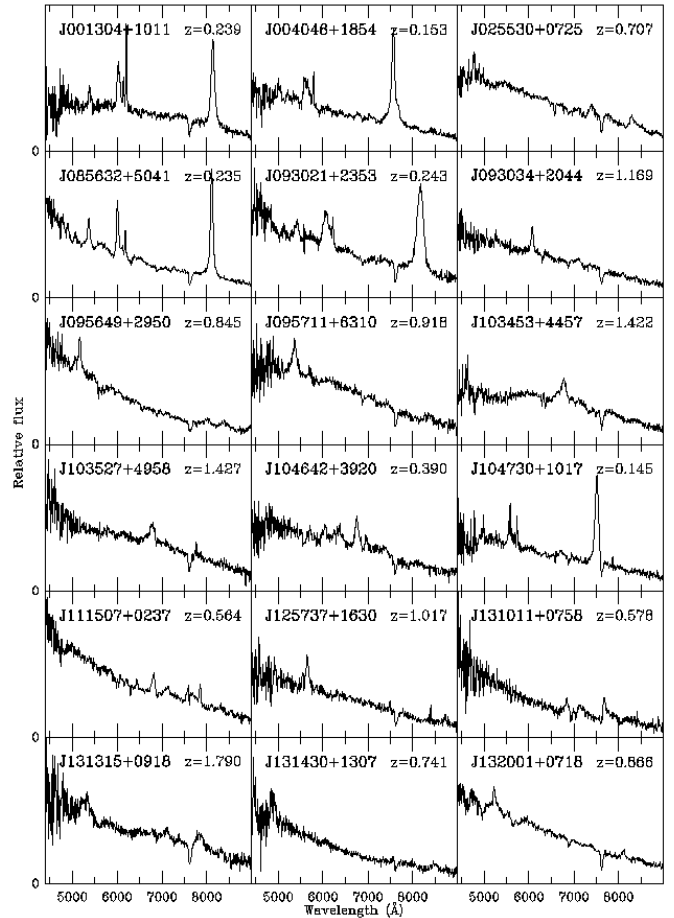**Fig. 11.** Spectrum of a cataclysmic variable observed at OAGH.

Fig. 12. Spectra of 18 QSOs from Table 4 observed at OAGH.

identifications (∼80%) and therefore we included all of them in our spectroscopic program.

In the case of starlike objects, the situation is more complex due to the facts that a large fraction of the X-ray sources are in fact X-ray stars and that, the surface density of stars being relatively large, there is a non negligible number of chance coincidences. The use of the O–E *vs.* O diagram turns out to be quite efficient to eliminate bright

Table 4. List of 103 QSO candidates identified with a ROSAT-FSC source and located in zone IVa. Col. 1: right ascension, col. 2: declination, col. 3: separation between the ROSAT and USNO positions in arcsec, col. 4: X-ray count rate (count s^{-1}), col. 5: magnitude O_{USNO}, col. 6: magnitude O_{APS}, col. 7: APS O–E colour, col. 8: redshift, col. 9: absolute O_{USNO} magnitude, col. 10: classification: DA, DN, WD: white dwarfs; *: stars; CV: cataclysmic variable; BL: BL Lac object; S1: Seyfert 1 galaxy; S1n: Narrow Line Seyfert 1; Q: QSO; col. 11: reference: (1) OAGH and (2) OHP observations, col. 12: name.

J2000 USNO position													
h	m	s	°	′	″	″	c/r	O_{US}	O_{APS}	O–E	z	M_{abs}		Ref.	Name
0	11	19.46	28	17	50.8	18.7	0.023	15.5	15.88	0.12			*	1	
0	13	4.80	10	11	28.6	5.8	0.023	16.0	16.25	0.32	0.239	−24.9	Q	1	
0	40	46.17	18	54	24.3	17.0	0.026	16.0	16.71	−0.12	0.153	−23.3	Q	1	
1	7	37.51	22	22	32.3	33.7	0.042	16.2	16.89	0.68			*	2	
1	20	46.96	23	31	40.1	28.7	0.047	15.9	16.27	0.54			*	2	
1	37	37.24	30	2	49.1	13.1	0.035	13.5	16.90	0.36			DN		TX Tri
2	55	30.70	7	25	57.1	19.4	0.030	16.3	16.97	0.66	0.707	−27.0	Q	1	
3	53	15.60	9	56	35.1	24.0	0.030	16.0	16.49	−0.82			*	2	
8	23	46.65	24	53	51.2	18.5	0.039	15.6	15.83	−0.40			WD	1	TON 316
8	39	34.28	23	34	10.4	12.8	0.041	15.8	16.49	−0.52			DA		PG 0836+237
8	45	51.14	60	9	13.7	13.3	0.027	16.0	16.30	−0.46			DA		PG 0841+603
8	50	20.09	54	33	50.5	17.3	0.038	16.4	16.78	0.62			*	1	
8	56	32.44	50	41	14.1	5.1	0.027	15.8	15.57	−0.58	0.235	−25.0	Q	1	
9	3	32.62	16	26	1.4	21.7	0.037	16.2	16.59	0.24			*	1	LB 9181
9	10	35.38	31	27	45.9	27.0	0.048	16.3	16.21	0.42			*	1	
9	10	37.97	53	12	2.8	19.3	0.030	16.4	16.82	0.52			*	1	
9	12	15.50	1	19	59.3	3.8	0.041	16.5	16.76	−0.50			*	1	
9	20	47.61	51	25	38.8	33.1	0.021	15.7	15.65	0.12			*	1	
9	30	6.76	52	28	4.0	12.0	0.039	15.8	16.37	−0.02			*		PG 0926+527
9	30	21.87	23	53	30.1	19.2	0.027	16.0	16.70	0.14	0.243	−24.3	Q	1	
9	30	34.46	20	44	16.9	5.2	0.045	16.1	17.09	0.64	1.169	−28.4	Q	1	
9	45	13.97	15	10	11.7	17.9	0.057	15.8	17.66	0.86			*	1	
9	46	34.50	13	50	58.3	34.4	0.027	15.8	16.75	0.10			CV	1	
9	49	39.77	17	52	49.5	12.0	0.021	16.3	18.65	0.60			DA		PG 0950+024
9	52	45.70	2	9	38.7	17.1	0.025	15.2	16.32	−0.76			DA		PG 0950+024
9	56	49.88	29	50	14.6	10.7	0.046	15.4	16.09	−0.10	0.845	−28.5	Q	1	TON 465
9	57	11.78	63	10	10.2	3.8	0.024	16.4	16.25	−0.06	0.918	−27.6	Q	1	
10	6	14.64	44	19	7.1	15.6	0.030	16.5	16.93	−0.30			DA		
10	34	53.07	44	57	23.1	20.5	0.023	16.1	16.57	0.38	1.422	−29.0	Q	1	
10	35	27.50	49	58	27.7	22.8	0.021	16.5	17.44	0.36	1.427	−28.5	Q	1	
10	44	19.33	19	57	47.9	24.2	0.039	15.6	15.90	0.44			*	1	
10	46	42.30	39	20	18.2	8.3	0.043	16.4	17.16	0.22	0.390	−25.3	Q	1	
10	47	30.55	10	17	28.9	17.7	0.228	15.4	15.81	0.08	0.145	−24.3	Q	1	
11	8	42.46	16	50	40.2	31.2	0.030	15.6	16.48	0.04			*	1	
11	14	1.95	52	27	11.6	29.8	0.023	15.5	15.62	0.40			*	1	
11	15	7.70	2	37	57.7	7.6	0.024	16.5	17.08	−0.04	0.564	−26.1	Q	1	
11	26	16.19	32	59	53.7	29.3	0.029	16.2	15.66	0.24			*	1	
11	33	31.23	58	57	47.8	19.9	0.025	15.9	15.98	0.44			*	1	
11	34	25.08	23	16	8.8	24.0	0.039	16.3	16.66	0.64			*	1	
11	38	36.32	47	55	10.0	13.3	0.046	16.1	17.53	−0.48			*	1	
11	41	52.82	25	35	33.5	10.8	0.042	16.3	16.82	−0.96			*	1	
11	47	47.34	26	0	49.0	10.9	0.042	15.5	15.84	0.00			*	1	
12	19	57.97	27	8	57.2	9.5	0.023	16.1	17.17	0.76			*	1	
12	31	25.72	25	55	59.8	5.7	0.032	15.8	16.16	0.54			*	1	
12	32	54.28	36	44	7.4	32.5	0.022	16.0	16.61	−0.08			WD	1	CBS 353
12	52	30.85	14	26	9.3	24.3	0.029	16.3	17.30	0.10					
12	57	37.02	16	30	48.6	13.5	0.035	16.1	16.95	0.66	1.017	−28.2	Q	1	
12	59	38.22	60	38	59.4	15.9	0.039	16.3	16.47	−0.48			*	1	SBS 1257+609
12	59	44.45	68	4	0.8	30.9	0.022	16.3	16.64	−0.72			*	1	FBS 1257+683
13	0	6.40	44	42	50.9	13.9	0.036	16.2	16.06	0.46			*	1	
13	10	11.30	7	58	16.5	21.2	0.030	15.8	16.52	−0.08	0.578	−27.0	Q	1	
13	13	15.90	9	18	20.4	27.7	0.021	16.4	17.34	0.10	1.790	−29.2	Q	1	
13	14	30.78	13	7	45.8	23.8	0.044	16.3	17.00	0.24	0.741	−27.1	Q	1	
13	20	1.10	7	18	17.1	21.1	0.038	16.5	16.97	0.74	0.866	−26.9	Q	1	
13	20	22.53	30	56	22.4	19.8	0.029	16.4	17.22	−0.04	1.587	−28.1	Q	1	US 583
13	24	47.70	3	24	32.9	15.5	0.040	16.5	16.84	0.54	0.303	−24.9	Q	1	

Table 4. (end)

	J2000 USNO position													
h	m	s	°	′	″	″	c/r	O_{US}	O_{APS}	O–E	z	M_{abs}		Ref.	Name
13	32	51.09	15	29	30.9	23.9	0.042	15.5	15.56	0.14			*	1	
13	33	45.80	5	38	42.6	22.2	0.028	15.5	15.74	0.10			*	1	
13	40	59.95	60	26	11.8	17.6	0.034	16.2	16.48	−0.68			DA		SBS 1339+606
13	42	46.90	18	44	43.8	22.4	0.039	16.4	16.69	0.12	0.382	−25.5	Q	1	
13	50	13.97	14	35	47.4	30.4	0.023	16.4	16.93	0.48			*	1	
13	51	25.25	19	5	33.4	10.8	0.027	16.4	16.89	0.64			*	1	
13	54	48.82	49	13	37.1	19.8	0.028	15.5	15.68	0.32			*	1	
13	55	43.99	20	12	31.8	19.9	0.030	15.6	16.11	0.30			*	1	
13	58	41.50	2	49	12.5	21.1	0.046	16.2	16.85	−0.08			*	1	
14	6	58.74	14	42	38.6	13.0	0.034	15.4	15.84	0.34	0.264	−25.7	Q	1	
14	9	39.24	28	16	49.9	25.2	0.035	16.1	16.93	0.34	0.165	−23.9	Q	1	
14	10	57.74	64	33	10.6	18.8	0.041	16.4	16.83	0.06	0.462	−25.9	Q	1	
14	17	30.16	13	0	1.6	11.6	0.021	15.7	16.00	0.38			*	1	
14	19	25.77	38	2	49.0	12.7	0.039	16.2	17.22	0.08	0.517	−26.3	Q	1	
14	31	10.98	14	23	8.3	3.7	0.022	16.1	15.91	−0.04	1.425	−29.0	Q	1	
14	47	50.12	38	5	30.3	12.2	0.023	15.8	16.28	0.04			*	1	
15	0	31.80	48	36	47.0	16.0	0.021	16.4	16.72	0.48	1.031	−27.9	Q	1	
15	5	27.62	29	47	18.7	8.7	0.036	15.0	15.65	−0.34	0.527	−27.6	Q	1	CSO 1080
15	8	32.28	67	42	43.4	9.0	0.032	16.0	17.12	0.14	0.336	−25.8	Q	1	
15	12	44.60	9	31	0.8	23.0	0.037	15.9	16.61	0.56			*	1	
15	16	32.30	12	13	50.5	10.6	0.028	16.2	17.26	0.78			BL	1	
15	44	3.76	26	48	38.6	21.7	0.023	16.4	17.15	0.74			*	1	
15	45	53.50	9	36	20.6	19.6	0.032	16.1	16.40	−0.22					
15	48	33.03	44	22	26.1	12.7	0.021	16.3	16.97	0.48	0.322	−25.2	Q	1	
15	51	9.60	45	42	52.1	22.5	0.036	15.6	15.95	0.32					
15	51	52.45	19	11	4.1	34.9	0.034	15.8	16.31	0.50					
15	53	4.93	35	48	28.6	25.2	0.033	16.1	17.20	0.72	0.722	−26.8	Q	1	
15	56	9.90	3	9	22.5	9.6	0.037	16.3	16.80	0.48	0.131	−23.2	S1n	1	
16	5	19.72	14	48	52.5	15.5	0.040	16.2	16.51	0.00	0.371	−25.7	Q	1	
16	9	47.80	7	12	33.2	27.8	0.021	16.4	16.95	0.64			*	1	
16	11	36.58	15	20	54.6	18.8	0.030	16.3	16.69	0.40	1.309	−28.6	Q	1	
16	17	42.10	6	2	23.8	20.4	0.078	15.5	15.69	0.42			*	1	
16	28	35.38	45	20	43.3	34.1	0.022	16.4	17.00	0.68			*	1	
16	30	9.65	45	16	37.9	21.7	0.022	16.5	16.96	0.32			*	1	
16	31	10.46	38	44	49.6	7.8	0.036	15.8	15.97	0.48			*	1	
16	45	20.15	61	35	9.7	3.8	0.023	16.4	16.89	0.64	0.410	−25.5	Q	1	
16	46	15.52	25	41	43.3	15.7	0.047	16.4	17.26	0.56	0.188	−23.9	Q	1	
17	18	28.97	57	34	22.3	6.4	0.039	15.9	16.07	0.48	0.100	−22.9	S1n	1	
17	20	13.19	49	55	26.4	28.8	0.027	16.0	15.89	0.36			*	1	
17	21	45.75	57	16	56.7	31.5	0.021	15.8	15.87	0.24			*	1	
17	28	13.44	32	22	5.8	10.8	0.022	16.4	17.08	0.34	0.563	−26.3	Q	1	
17	29	35.53	52	30	47.5	3.0	0.029	16.2	15.96	0.02	0.278	−25.0	Q	1	
17	49	12.30	55	12	8.9	28.7	0.023	16.3	16.58	0.44			WD	1	
22	37	31.84	10	19	4.0	3.8	0.024	16.5	16.77	−0.46	0.103	−22.5	S1	1	
22	37	33.28	10	18	42.7	26.3	0.024	15.9	16.10	0.50			*	1	
23	7	13.30	4	32	2.5	29.8	0.079	15.9	17.25	−0.92			*	1	
23	15	52.73	11	33	2.1	21.4	0.036	16.5	17.20	0.24	0.567	−26.2	Q	1	KUV 23134+1117

stars and late type stars. However, although in our region IVa most objects are genuine identifications, in zones IVb and III there are many chance coincidences with main sequence stars. The use of the Hamburg slitless spectra in these zones is crucial to separate QSOs from stars. In addition, Seyfert 1 galaxies are often compact and classified as starlike in the APS. Moreover they usually have a relatively red O–E colour; as a consequence they easily escape detection by our automatic procedure and classification on the basis of the slitless spectra is necessary.

The relatively poor positional accuracy of the ROSAT survey ($\sigma \sim 15''$) makes it difficult to identify objects weaker than ~ 16.5; but this limiting magnitude is well fitted by the magnitude limit below which no recognition
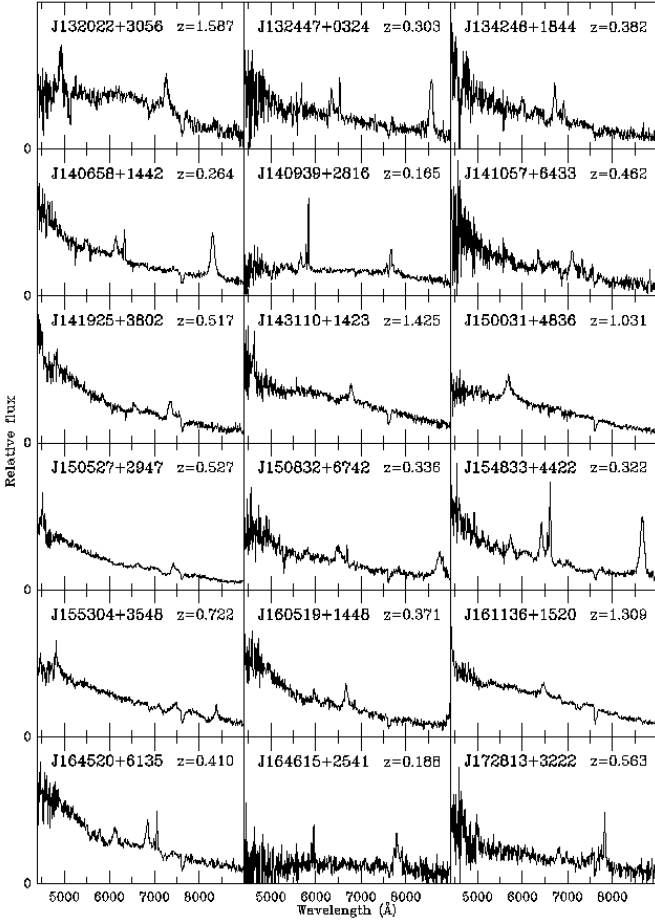
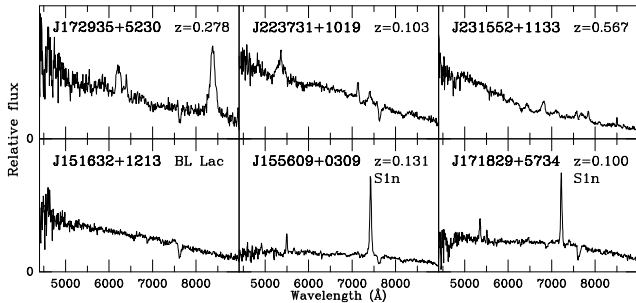**Fig. 13.** Spectra of 18 QSOs from Table 4 observed at OAGH.

Fig. 14. Spectra of six objects from Table 4 (one Seyfert 1, one QSO, two BL Lac objects and two NLS1s) observed at OAGH.

of absorption features is possible in the Hamburg slitless spectra.

5.2. Completeness of our QSO sample

We have seen that only 85% of the bright USNO objects have a counterpart in the APS due mainly to the incompleteness of the data base. Moreover only 60% of the known QSOs fall into our zone IVa to which we have restricted our search. Therefore our sample is expected

to be no more than 50% complete.

On the other hand, as our aim is to find all AGN brighter than a given optical magnitude, we have to answer the following question: how many such AGN are missed if we identify all bright AGN in a flux limited X-ray survey?

Table 5. Number and percentage of radio quiet and radio loud X-ray detected QSOs in the Véron-Cetty & Véron catalogue. Cols. 1 and 2: O_{USNO} range, col. 3: number of QSOs, col. 4: number of sources brighter than 0.02 count s^{-1} in the ROSAT catalogues, col. 5: percentage of ROSAT detected QSOs; col. 6 to 8: the same for the radio loud QSOs.

		Radio quiet			Radio loud		
O_{min}	O_{max}	n	n_X	%	n	n_X	%
	<15.5	80	58	72	9	7	78
15.5	16.0	90	48	53	21	17	81
16.0	16.5	243	101	42	49	37	76
16.5	17.0	433	144	33	99	60	61
17.0	17.5	679	101	15	172	77	45
17.5	18.0	900	60	7	201	59	29
18.0	18.5	977	23	2	169	41	24
18.5	19.0	1040	13	1	107	11	10
19.0	19.5	475	4	1	41	5	12
19.5	20.0	87	0	0	18	5	28

The current version of the Véron & Véron QSO catalogue contains 5 893 QSOs at $\delta > 0°$, $|b| > 30°$, with B<20.0 and z>0.10, found in the course of radio or optical surveys (QSOs found as the identification of a X-ray source have been ignored). Of these, 871 are located within 35″ from a ROSAT-BSC or -FSC source (stronger than 0.02 count s^{-1}). We consider them as genuine identifications; 319 are radio loud and 552 radio quiet.
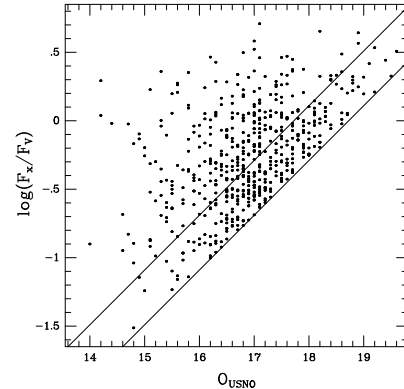
Fig. 15. Plot of $\log(F_X/F_V)$ *vs* O_{USNO} for 552 radio quiet QSOs. The two diagonal lines correspond to the sensitivity limits of the BSC and FSC ROSAT survey (0.05 and 0.02 count s^{-1}, respectively).

On average, QSOs with higher optical luminosity have higher X-ray luminosity. According to Maccacaro et al. (1988), $\log(F_X/F_V)=\log(F_X)+0.4\times V+5.37$ where F_X is the X-ray flux in the 0.3-3.5 keV band in erg cm^{-2} s^{-1} and $F_V=-0.4\times V-8.42$ is the flux in the V band in the same units. For the ROSAT survey, this translates into: $\log(F_X/F_V)=\log($PSPC counts s$^{-1}\times10^{-11})+0.4\times V+5.37$ where F_X is the X-ray flux in the 0.1-2.4 keV band, assuming a conversion factor of 1 PSPC count s^{-1} for a flux of 10^{-11} erg cm^{-2} s^{-1} in this band which corresponds to an unabsorbed source with a photon index $\Gamma=2.3$, a typical value for QSOs (Voges et al. 1999).

Fig. 15 shows $\log(F_X/F_V)$ *vs* O_{USNO} for the 552 radio quiet QSOs. Table 5 gives the fraction of ROSAT detected QSOs *vs* their optical magnitude for both the radio quiet and the radio loud samples.

At $O_{USNO}=16.0$, about half of the optically selected QSOs are not detected in X-ray (Table 5) and therefore have $\log(F_X/F_V)<-1$. Consequently the median value of their X-ray to optical flux ratio is ~-1.0. Figure 15 suggests that $\sigma\sim0.5$.

Zickgraf et al. (2003) found that the median value of $\log(F_X/F_V)$ for X-ray selected QSOs is 0.39. The fact that these objects are significantly stronger X-ray sources than optically selected QSOs is due to the much higher frequency of the survey. Indeed Williams & Bridle (1967) and Kellermann et al. (1968) have shown that the relative numbers of sources with given spectral indices depend on the frequency at which the sample is selected. A sample selected at a low frequency (optical) will include a greater proportion of sources with high values of the spectral index than will a similar sample selected at a high frequency (X-ray).

In the simple case where the distribution of the spectral indices α in a complete sample of sources selected at a wavelength λ_o is Gaussian with a mean spectral index α_o and a standard deviation σ_α, the distribution of the spectral indices of sources selected at another wavelength λ_X will also be Gaussian with the same standard deviation σ_α, but with a mean spectral index α_X given by:

$$\alpha_X=\alpha_o+\mu\times\sigma_\alpha^2\times\ln(\lambda_X/\lambda_o).$$

In this expression μ is the exponent in the population law $N(S)\sim S^{-\mu}$ giving the number of sources with flux densities in excess of a specified value S (Williams & Bridle 1967). With $\mu=1.87$, $\lambda_o=5\,000$ Å and $\lambda_X=12.4$ Å (1 keV), we find that to get the observed increased value of F_X/F_V by a factor 25, corresponding to $\alpha_X-\alpha_o=0.54$, a value of $\sigma_\alpha=0.22$ is required, *i.e.* $\sigma=0.57$, where $\sigma=2.60\times\sigma_\alpha$ is the standard deviation of $\log(F_X/F_V)$. This is in reasonable agreement with our estimated value of $\sigma\sim0.5$.

Table 5 confirms that radio loud QSOs are brighter X-ray sources than radio quiet QSOs. In addition we found that, for BL Lac objects, the mean F_X/F_V ratio is larger than that of the radio loud QSOs as previously shown by Stocke et al. (1985). BL Lac brighter than 15.5 are all detected by ROSAT while at $O_{APS}=20.0$, 50% are still detected.

5.3. The surface density of bright QSOs

The surface density of bright QSOs is difficult to determine because these objects are rare and therefore large areas of the sky have to be surveyed to find a substantial number. The Bright QSO Survey (BQS) of Schmidt & Green (1983) covering 10 714 deg^2, contains 69 QSOs brighter than $M_B=-24.0$ and B=16.16, corresponding to 0.0064 ± 0.0008 deg^{-2}. A number of works suggest that this value is substantially underestimated and that the completeness of the BQS is in the range 30%-70% (Wampler & Ponz 1985; Goldschmidt et al. 1992; La Franca & Cristiani 1997; Wisotzki et al. 2000; Mickaelian et al. 2001).

Grazian et al. (2002) have undertaken a program similar to ours. They cross-correlated the ROSAT-BSC with the Digitized Sky Survey in the southern hemisphere to find all coincidences between X-ray sources and stellar objects brighter than $B_J<15.13$. After spectroscopic observations of the candidates, they obtained a sample of 111 AGN in an area of 5 660 deg^2, 57 being brighter than $M_B=-24.0$. But the distribution of absolute magnitudes is rather odd, 46 being greater than –25.0 and 5 smaller than –26.0. We checked the appearance of some of the low redshift objects on the DSS images; they are clearly galaxies; their O magnitude in the APS data base is much greater than the B magnitude given by Grazian et al. and the absolute magnitudes computed with these O magnitudes are definitely greater than –24.0. The true number of QSOs in this sample is therefore unknown, but certainly significantly smaller than 57.

There are, in our region of interest (10 313 deg^2), 503 known QSOs ($M_B<-24.0$ *i.e.* $M_O<-24.4$) brighter than $O_{USNO}=16.5$, *i.e.* B=16.9 (on the average, the O_{USNO} magnitudes are brighter than the photoelectric B magnitudes: $<O_{USNO}-B>=-0.38$; Mickaelian et al. 2001). 191 are associated with a BSC source, 84 with a FSC source and 228 are not detected by ROSAT. Here we use USNO rather than APS O magnitudes because the selection has been made with the USNO data base; using the APS magnitudes, our sample would not be complete to O=16.5.

These 503 QSOs correspond to a surface density of 0.041 ± 0.002 QSO deg^{-2} brighter than B=16.9. If the integrated number-magnitude relation has a slope equal to $b=\mu/2.5=0.75$ (Sandage & Luyten 1969), the surface density of QSOs brighter than B=16.16 is 0.0114 deg^{-2}. Of these QSOs 142 are brighter than $O_{USNO}=15.8$ (B=16.2), corresponding to 0.014 ± 0.001 deg^{-2}, in agreement with the preceding value, confirming that the value of b used is reasonable.

The QSO counts are systematically affected by the photometric errors on the magnitudes as these errors scatter many more objects toward bright magnitudes than it does toward faint magnitudes. Assuming that the error

distribution is Gaussian, with a dispersion σ, the correction to be applied to the observed counts is a factor $10^{(b+1)\sigma^2/2}$ (Eddington 1940). With b=0.75 and σ=0.31, the true QSO surface density is smaller by 1.21 than the observed one or, at B=16.16, 0.011±0.002 deg^{-2}. This is already 78% larger than the original Schmidt & Green estimate.

Sixty seven of the known QSOs ($M_O<-24.4$) with available APS magnitudes are associated with a ROSAT-FSC source, 35 being located in zone IVa (Table 3). In this zone, we have found 33 additional such objects (see Table 4), almost doubling the number of known QSOs at this limiting magnitude.

We should note in addition that, among the 84 EBL-WK objects, 14 have not yet been spectroscopically observed, while 5 of the QSOs candidates in Table 4 have still to be observed. This may increases the number of new bright QSOs.

6. Conclusion

We have undertaken a program of systematic identification of optically bright AGN in both the BSC- and FSC-ROSAT catalogues. In this paper we present preliminary results concerning the FSC catalogue. We describe the method used which consists of first cross-correlating the USNO and APS databases with the X-ray catalogue, then checking the nature of the candidates by looking at the slitless Hamburg spectra.

Among the starlike objects brighter than B=16.9 we have recovered 35 previously known QSOs in the region of the O/(O–E) diagram containing 60% of the bluest QSOs and discovered 33 new ones confirming that, even at these relatively bright magnitudes, available surveys are significantly incomplete.

The total number of previously known QSOs brighter than B=16.2 corresponds to a surface density 78% higher than the original Schmidt & Green value. But we have shown that, in the subsample studied here *i.e.* the QSOs associated with a ROSAT-FSC source, the completeness is at best 50%. Although we cannot generalize this to the whole sample, it is not unlikely that the true surface density is significantly higher than the number derived here.

We found that at this magnitude and at a flux limit of 0.02 counts s^{-1}, only 40% of all QSOs are detected by ROSAT.

7. Acknowledgments

References

Bade N., Engels D., Voges W. et al. 1998, A&AS 127,145
Cabanela J.E., Humphreys R.M., Aldering G. et al. 2003, PASP 115,837
Comastri A., Brusa M., Mignoli M. & Hellas team 2003, AN 324,28
Condon J.J., Yin Q.F., Thuan T.X. & Boller T. 1998, AJ 116,2682
Eddington A.S. 1940, MNRAS 100,354
Goldschmidt P., Miller L., La Franca F. et al. 1992, MNRAS 256,65P
Grazian A., Omizzolo A., Corbally C. et al. 2002, AJ 124,2955
Hagen H.-J., Groote D., Engels D. & Reimers D. 1995, A&AS 111,195
Hornschemeier A.E., Brandt W.N., Garmire G.P. et al. 2001, ApJ 554,742
Hornschemeier A.E., Bauer F.E., Alexander D.M. et al. 2003, AJ 126,575
Kellermann K.I., Pauliny-Toth I.I.K. & Davis M.M. 1968, Astrophysical letters 2,105
Klemola A.R., Jones B.F. & Hanson R.B. 1987, AJ 94,501
La Franca F. & Cristiani S. 1997, AJ 113,1517
Laor A., Fiore F.,Elvis M., Wilkes B.J. & McDonnel J.C. 1997, ApJ 477,93
Lasker B.M., Doggett J., McLean B. et al. 1996, ASP Conf. Ser. 101,88
Lemaître G., Kohler D., Lacroix D., Meunier J.-P. & Vin A. 1989, A&A 228,546
Maccacaro T., Gioia I.M., Wolter A., Zamorani G. & Stocke J.T. 1988, ApJ 326,680
Mickaelian A.M., Gonçalves A.C., Véron-Cetty M.-P., & Véron P. 1999, Astrophysics 42,5
Mickaelian A.M., Gonçalves A.C., Véron-Cetty M.-P. & Véron P. 2001, Astrophysics 44,21
Monet D., Bird A., Canzian B. et al. 1996, USNO-A2.0, U.S. Naval Observatory, Washington D.C.
Moran E.C., Halpern J.P., & Helfand D.J. 1996, ApJS 106,341
Odewahn S.C., Stockwell E.B., Pennington R.L. & Humphreys R.M. 1992, AJ 103,318
Röser S. & Bastian U. 1991, PPM star catalogue, Astronomisches Rechen-Institut Heidelberg
Sandage A. & Luyten W.J. 1969, ApJ 155,913
Schmidt M. & Green R.F. 1983, ApJ 269,352
Schwope A.D., Hasinger G., Lehmann I. et al. 2000, AN 321,1
Severgnini P., Caccianiga A., Braito V. et al. 2003, A&A 406,483
Stocke J.T., Liebert J., Schmidt G. et al. 1985, ApJ 298,619
Tananbaum H., Avni Y., Branduardi G. et al. 1979, ApJ 234,L9
Véron-Cetty M.-P. & Véron P. 2001, A&A 374,92
Voges W., Aschenbach W., Boller T. et al. 1999, A&A 349,389
Voges W., Aschenbach W., Boller T. et al. 2000, IAU Circ. 7432

Wampler E.J. & Ponz D. 1985, ApJ 298,448

Williams P.J.S. & Bridle A.H. 1967, The Observatory 87,280

Wisotzki L., Christlieb N., Bade N. et al. 2000, A&A 358,77

Zickgraf F.-J., Thiering I., Krautter J. et al. 1997, A&AS 123,103

Zickgraf F.-J., Engels D., Hagen H.-J., Reimers D. & Voges W. 2003, A&A 406,535